ISSN (e): 2250 – 3005 || Volume, 05 || Issue, 06 || June – 2015 ||
International Journal of Computational Engineering Research (IJCER)

Using Computational Fluid Dynamics as a tool for improved prediction of pressure characteristics of a pilot chamber of PRSOV

Binod Kumar Saha [1], Dipankar Sanyal [2]
[1] *Product Design and Simulation Division,*
CSIR-Central Mechanical Engineering Research Institute, Durgapur – 713209, India,
[2] *Department of Mechanical Engineering, Jadavpur University, Kolkata – 700032*

ABSTRACT:
In this paper, flow of air through a pressure regulating and shut-Off Valve (PRSOV) has been solved numerically with an objective to determine the pressure of the PRSOV pilot chamber. Flow through the valve is transient, compressible and turbulent in nature. Flow has been solved using ANSYS FLUENT coupled with a special user defined function (UDF). UDF is used for dynamic meshing, automatic data acquisition from ANSYS FLUENT solver and to schedule the numerical test procedure. Within the UDF, valve inlet pressure is varied in a stepwise manner. For every value of inlet pressure, transient analysis leads to a quasi-static flow through the valve. Spool forces are calculated based on different pressures at inlet. From this information of spool forces, pressure characteristic of the pilot chamber of passive control circuit has been derived. The same characteristics have also been obtained after modelling the flow analytically. Both the results have been compared. It is observed, CFD analysis of the flow has led to improved results.

KEYWORDS: *Pressure regulating and Shut-Off Valve, pilot flow, dynamic meshing, flow force, pressure regulation, Force Balance, CFD*

I. INTRODUCTION

Pressure regulating and Shut-off valve is a critical component used in many fluid power systems, especially in aircraft. The valve is used in Environmental Control System of the aircraft. The valve is installed in a pipe line in an air flow path where available inlet pressure to the valve may vary within a wide range. The main function of the valve is to regulate the air flow and maintain almost constant pressure at its outlet. Schematic diagram of the valve is shown in Fig. 1.

A passive control circuit (Pilot chamber pressure control circuit in Fig. 1) is required to achieve the above objective. Depending upon the valve inlet pressure, this passive control circuit sets the criterion for position of spool inside the valve. Determination of characteristics of the control circuit is a crucial part in designing the control circuit and hence the pressure regulated valve. This requires complete information of flow forces acting on the valve spool. Calculations based on theoretical model can provide some initial approximate information. With the advent of numerical power, advanced, sophisticated and reliable CFD tool is very useful in determining the various flow forces acting on the spool.

Leutwyler and Dalton [1] showed the potential of CFD tool in analyzing compressible, turbulent flow through butterfly valves. ANSYS FLUENT was used for the analysis. Amirante et al. [2-3] evaluated flow forces on an open centre direction control valve. Amirante et al. [4] again modelled direct proportional valve using CFD. Compensation techniques based on spool profiling were used to balance the flow force at different level of valve openings. Chen et al. [5] reported flow visualization using CFD in a ball valve. Chattopadhyay et al. [6] have investigated turbulent flow structure inside a Pressure Regulating and Shut-Off Valve using ANSYS FLUENT. In this work, both 2-D and 3-D simulations were performed with a conclusion that 2-D model could predict the flow coefficients satisfactorily. Song et al. [7] have reported 2D dynamic simulation of a pressure relief valve using CFD.

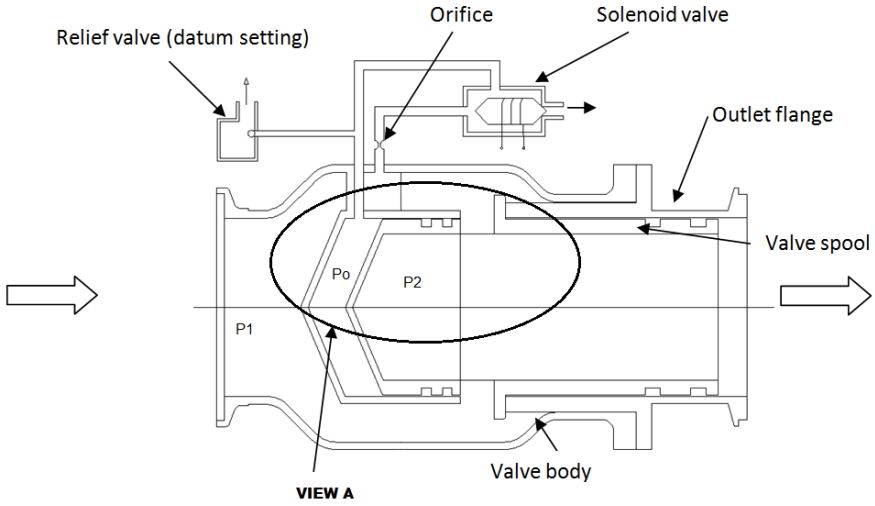

Fig. 1. Schematic diagram of pressure regulated valve

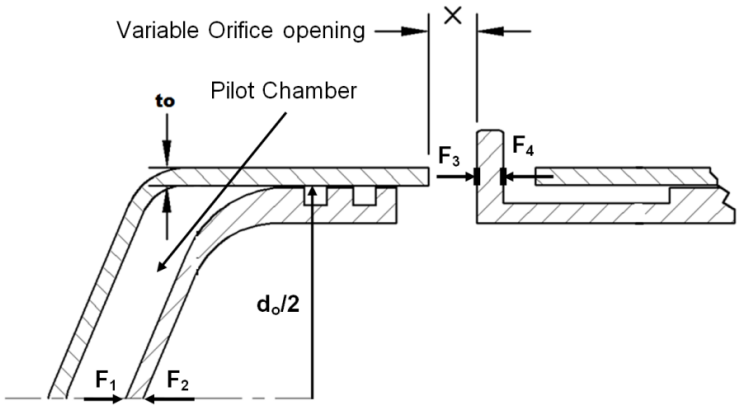

View A

In this study, transient, compressible and turbulent flow through a pressure regulated valve has been solved using commercial software ANSYS FLUENT [10]. As the valve inlet pressure changes, spool inside the valve as shown in Fig. 1 must move in appropriate direction to keep outlet pressure constant. Starting from the instant of inlet pressure change, a transient analysis is performed to reach the state of quasi-static flow through the valve.

II. ANALYTICAL METHOD

Pressure Regulating and Shut-Off Valve (PRSOV) consists of valve body, spool and pilot chamber. Inlet pressure (P_1) of the valve may vary from 207 kPa to 758 kpa. Main function of the valve is to keep the outlet pressure (P_2) at almost constant value. Spool inside the valve body is subjected to a number of forces. When there is a change in inlet pressure, spool moves in appropriate direction and outlet pressure should remain almost constant value.

2.1 Force balance on the spool

spool moves under the action of four forces, F_1, F_2, F_3 and F_4 as shown in Figure1. Force F_1 arises due to the pilot chamber air pressure (P_o). Pilot chamber air pressure is controlled by datum setting of relief valve as shown in Fig. 1. The effective area on which this pilot pressure acts is $\pi d_o^2/4$. Therefore, $F_1 = P_o \times \frac{\pi d_0^2}{4}$ and acts from left to right direction as shown in Figure1.

As the high pressure air flows through the variable orifice, air pressure reduces from inlet pressure (P_1) to outlet pressure (P_2). This outlet pressure acts on the other side of the spool head. Thus a force (F_2) acts on the spool from right to left direction as shown in Fig. 1. Here, $F_2 = P_2 \times \frac{\pi d_0^2}{4}$.

Air pressure changes from P_1 to P_2 as it flows through the orifice. Orifice is formed by spool flange and the valve body thickness (t_o). Since t_o is small enough, so pressure variation is assumed linear. Therefore, average pressure $(P_1 + P_2)/2$ acts on spool flange over an annular area with diameter $(d_o + t_o)$ and thickness t_o.

Here the force, $F_3 = \frac{(P_1+P_2)}{2} \times \pi(d_o + t_o) \times t_o$. Since t_o is small value, so higher order term of t_o can be neglected. Then, $F_3 = \frac{(P_1+P_2)}{2} \times \pi d_o \times t_o$ and the force (F_4), which acts on similar area on the other side of the spool flange, is given as $F_4 = P_1 \times \pi d_o \times t_o$.

Spool remains at equilibrium state under the action of these four forces. Therefore, $F_1 + F_3 = F_2 + F_4$

or, $P_o \times \frac{\pi d_0^2}{4} + \frac{P_1+P_2}{2} \times \pi d_0 \times t_o = P_1 \times \pi d_o \times t_o + P_2 \times \frac{\pi d_0^2}{4}$

or, $P_o = \frac{t_o}{2d_o} \times P_1 + \left(1 - \frac{t_o}{2d_o}\right) \times P_2$.

III. CFD METHOD

3.1 Mathematical modelling

The ANSYS FLUENT package has been used to solve the axisymmetric flow in the domain shown in Fig. 2. The partial differential equations for the conservation of mass, momentum, energy, turbulence kinetic energy k and turbulence dissipation rate ε along with the algebraic equation for the perfect gas laws have been solved. As given below, these involve time t as the independent variable, the dependent variables of density ρ, velocity $\bar{v}$, pressure p, temperature T and the flow parameters of kinematic viscosity ν_l, turbulent viscosity ν_t, molecular diffusivity α_l and turbulent diffusivity α_t.

Mass conservation equation: $\partial\rho/\partial t + \nabla.(\rho\bar{v}) = 0$,

Momentum conservation equation:

$$\partial(\rho\bar{v})/\partial t + \nabla.(\rho\bar{v}\bar{v}) = -\nabla p + \rho(\nu_l + \nu_t)\nabla.\{\nabla\bar{v} + (\nabla\bar{v})^T - (2\bar{\bar{I}}/3)\nabla.\bar{v}\},$$

Energy conservation equation:

$$\partial T/\partial t + \bar{v}.\nabla T = -(\alpha_l + \alpha_t)\nabla^2 T + (\nabla\bar{v}):[\rho(\nu_l + \nu_t)\{\nabla\bar{v} + (\nabla\bar{v})^T - (2\bar{\bar{I}}/3)\nabla.\bar{v}\}],$$

Turbulence Kinetic Energy Equation:

$$\partial(\rho k)/\partial t + \nabla.(\rho\bar{v}k) = \nabla.[\rho(\nu_l + \nu_t/\sigma_k)\nabla k] + G_k - \rho\varepsilon - 2\rho\varepsilon k/(\gamma RT),$$

Turbulence Dissipation Equation:

$$\partial(\rho\varepsilon)/\partial t + \nabla.(\rho\bar{v}\varepsilon) = \nabla.[\rho(\nu_l + \nu_t/\sigma_k)\nabla\varepsilon] + \rho C_1 S\varepsilon - \rho C_2\varepsilon^2/(k + \sqrt{\nu\varepsilon}),$$

where $S = [\{\nabla\bar{v} + (\nabla\bar{v})^T\}:\{\nabla\bar{v} + (\nabla\bar{v})^T\}/2]^{1/2}$,

$G_k = \mu_t S^2$,

C_1 and C_2 are constants and σ_k and σ_ε are turbulent Prandtl number respectively, R is the gas constant and γ is the specific heat ratio. Consistent with the realizable k-ε model due to Shih et al. [13], the equations and the values of the different parameters are chosen as

$\upsilon_t = C_\mu k^2/\varepsilon$,

$\alpha_t = \nu_l.\nu_t/(\alpha_l \Pr_t)$,

and $\mu = \mu_o(T/T_o)^{3/2}\{(T_o + s)/(T + s)\}$,

where μ_o and T_o are reference viscosity and temperature, s is Sutherland constant and $\Pr_t$ is the turbulent Prandtl number, which have been taken respectively as equal to 1.716 x 10-5 Pa-s, 273.11 K, 110.56 K and 0.85.

3.2 Boundary Conditions

Following boundary conditions were used for this analysis.

1. Inlet boundary where a fixed pressure condition is used. The inlet temperature is fixed at 633 K.
2. As discussed above, outlet boundary of the flow domain is open to ambient. So, pressure and temperature have been set to 101325 Pa and 298.15 K, respectively.
3. No-slip boundary condition is assigned for all the walls. The valve wall was assumed to be at adiabatic condition.
4. For prescribing turbulent quantities at the boundaries, several options are available. We have used a condition prescribing the level of turbulent intensity (TI) at around 5-10% in the incoming fluid stream which is a reasonable level of value used by researchers. Hydraulic diameter of 47.5mm in the incoming fluid stream has been considered.

The initial conditions are the steady state result corresponding to the pressure p_1 at the inlet of the valve body equal to 207 kPa and all other boundary conditions as stated above.

Flow geometry has been approximated with a 2D axisymmetric domain as shown in Fig. 2. Unstructured quadrilateral mesh has been generated using commercial software package ANSYS ICEM CFD. Dynamic mesh motion along with the movement of spool boundaries has been considered during mesh generation. Entire fluid flow domain has been divided into two parts as shown in Fig. 3. Mesh for zone 1 does not possess any motion, whereas mesh for zone 2 undergoes dynamic motion. Wall boundaries comprising spool surfaces move depending upon the conditions as mentioned in FLOWCHART in Fig. 5. Some of the internal edges also move with spool surfaces. One special internal edge has been selected to move with spool surfaces but at exactly half the speed of spool movement. This special movement serves a very important purpose; finer boundary layer of the variable orifice remains intact though the spool opening reduces. Initial mesh contains 0.2 million quadrilateral cells approximately.

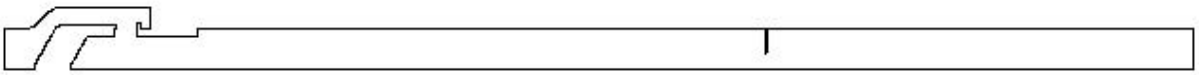

Fig. 2. 2D axi-symmetric flow domain

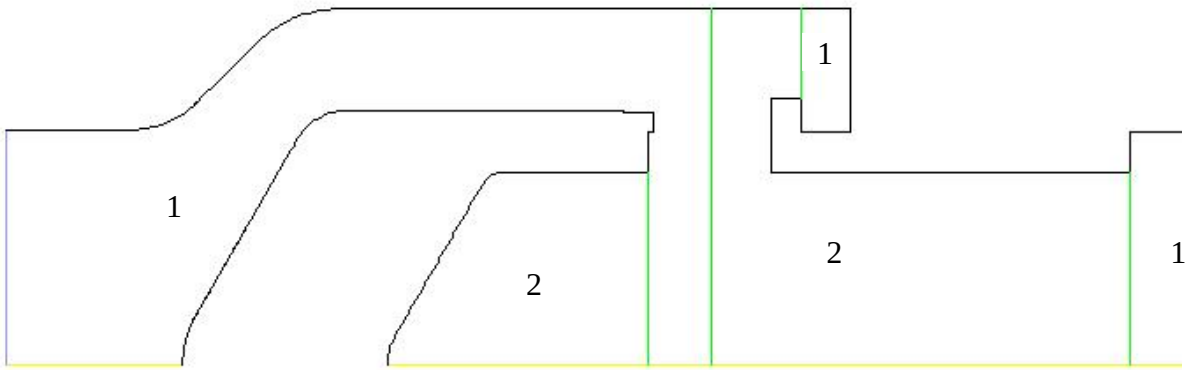

Fig. 3. Flow domain showing two different zones of fluid

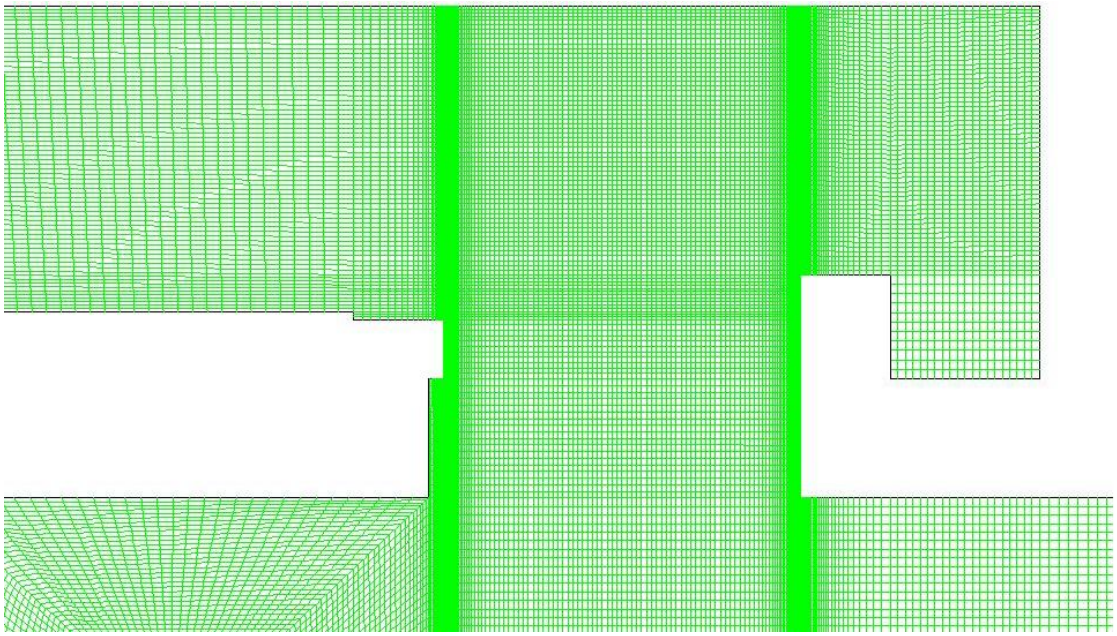

Fig. 4. Structured quadrilateral mesh around orifice opening

3.4 Methodology of calculation

Valve inlet pressure may vary from 207 kPa to 758 kPa, whereas valve outlet pressure remains within 200 kPa to 241 kPa. Air flow further downstream of valve outlet is approximated with the help of an orifice flow finally open to ground level condition. Calculation domain, therefore, includes the valve geometry along with the appropriate pipe length before and after the orifice. 2D axisymmetric flow geometry is shown in Fig. 2.

Transient flow through this flow domain is solved in ANSYS FLUENT to determine various spool openings depending on various inlet pressures. Now, when the inlet pressure is at the minimum value, i.e., 207 kPa, spool opening should be 100%. Therefore, solution of this flow sets the initial condition for transient calculation. In transient calculation, inlet pressure is varied in a step wise manner. This is done via a User Define Function (UDF). In reality, when inlet pressure is changed by a small amount, flow through the valve will take some time to die down the transient phenomena. In CFD, this quasi-static state is achieved after solving the transient flow for a number of time steps. For each time step, the flow convergence is checked using UDF that allows the calculation to move to next time step only after meeting the required criteria for convergence. Also, a check, whether quasi-static condition has been achieved, is carried out with the help of same UDF before proceeding to next time step. This UDF is described with the help of a FLOWCHART given in Fig. 5.

When the transient dies down pressure at valve outlet is checked for the desired outlet pressure. If desired pressure is not obtained, then spool opening is reduced by a delta amount and further transient calculation is carried on. This whole process is automated using the UDF. When the desired pressure is obtained, UDF directs ANSYS FLUENT to write the Case and Data file for further post processing. Spool opening and valve outlet pressure for each time step are written in a DAT file with the instruction written in UDF. This file is required for further reference. After achieving the desired pressure at valve outlet, UDF directs ANSYS FLUENT to increase the valve inlet pressure by a small amount and again the whole loop of operations repeated.

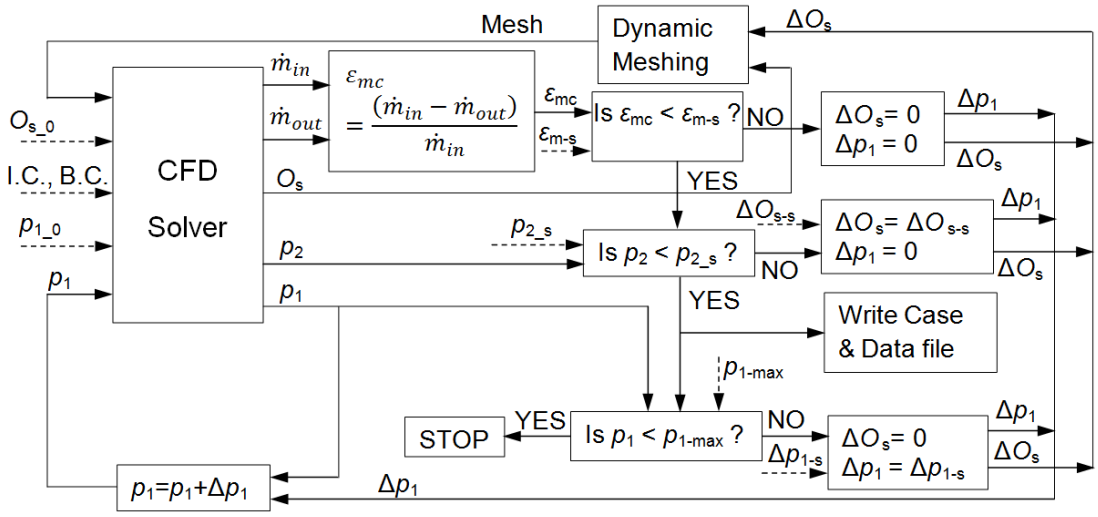

Fig. 5. FLOWCHART for special UDF

IV. RESULTS AND DISCUSSION

Flow through the pressure regulated valve is governed by variable orifice flow. Fig. 6 shows the spool opening in mm against the gauge pressure at valve inlet. It is observed here that spool opening reduces by 86% as valve inlet pressure increases from 240kPa to 360kPa. Thereafter, the gradient of change in spool opening with inlet pressure is very slow. This happens because pressure is almost fixed at valve outlet.

Fig. 7 shows the variation of mass flow rate with the change in inlet pressure. There is no significant change in mass flow rate. This is justified as two things happen simultaneously.

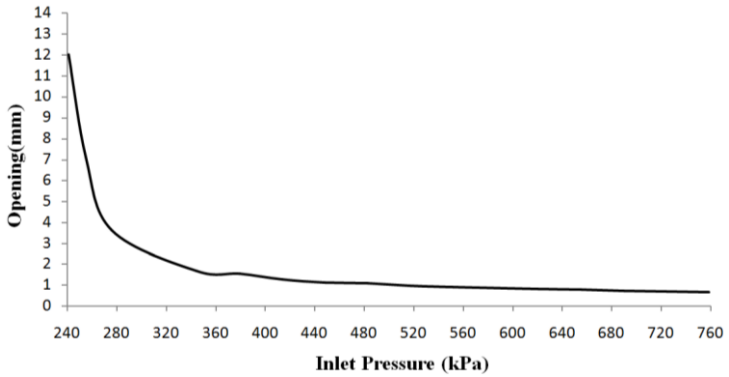

Fig. 6. Spool opening plotted against valve inlet pressure.

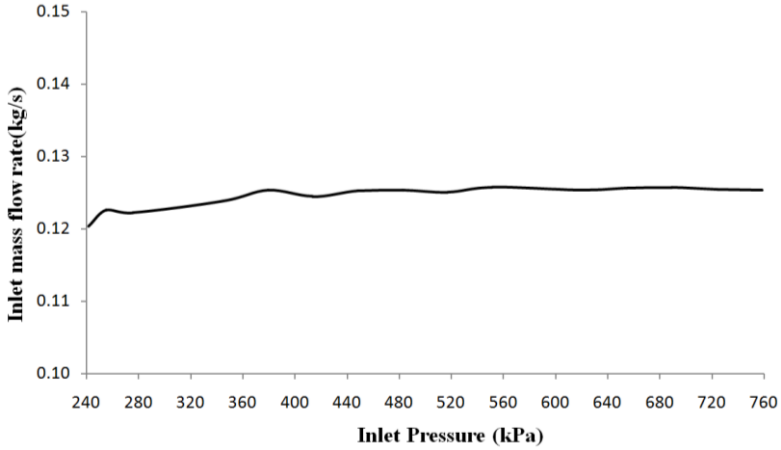

Fig. 7. Variation of mass flow rate through valve with change in inlet pressure.

Resistance in flow path increases as spool opening reduces, which would try to decrease mass flow rate. However, the increase in inlet pressure almost nullifies the above effect.

In Fig. 8 flow forces acting on spool surfaces are plotted against the inlet pressure. The force is acting axially from right to left direction with respect to Fig. 1. Both analytical and CFD results are plotted here. In both the cases, it is observed that the net force increases with increase in the inlet pressure. This owes to the fact that the spool opening creates an orifice and the air pressure acting on the orifice side of spool flange is less than the pressure that acting on the outer side of the spool flange. The derivation in Section 2.1 makes this aspect clearer. Higher absolute force is predicted by the CFD analysis. This pressure distribution and the consequent prediction of spool force is of course more realistic in view of the more detailed nature of the CFD analysis in comparison to a lumped calculation.

As the spool is subjected to a flow force from right to left, a counter force is required to keep the spool at the desired location. This force comes from pilot chamber air pressure. Air pressure in the pilot chamber is maintained by a Pilot Chamber Pressure Control circuit. There is a spring loaded Pressure Relief Valve in that circuit. The required pilot pressure to balance the spool is calculated and plotted in Fig. 9. Both Fig. 8 and Fig. 9 show that CFD analysis has led to sufficient improvement of the pilot chamber pressure characteristic with respect to the analytical results.

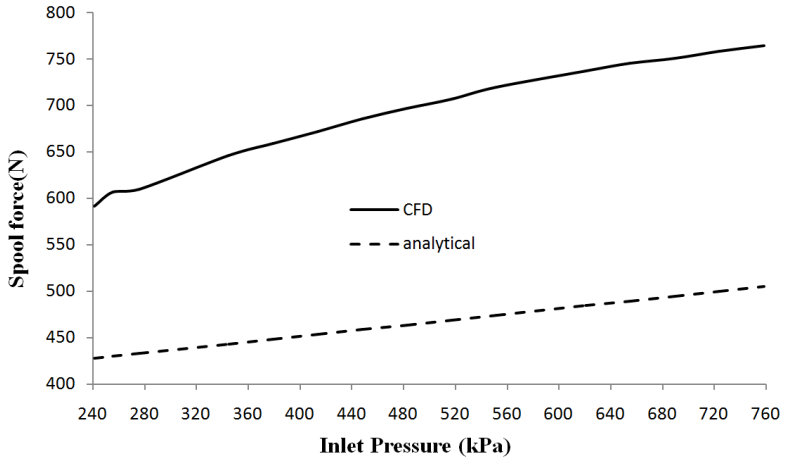

Fig. 8. Variable flow forces on spool surfaces with inlet pressure variation.

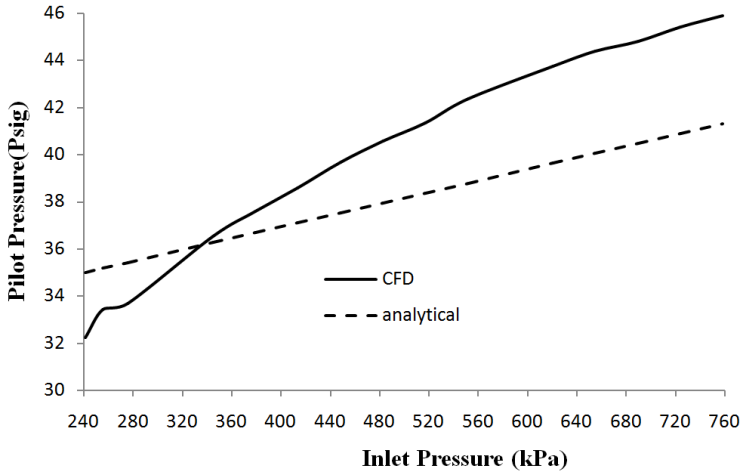

Fig. 9. Pressure characteristic of passive control circuit.

Fig. 10 shows the contour plots of static pressure at 100%, 60%, 30% and 10% spool opening. Corresponding inlet pressures are 241 kPa, 255 kPa, 276 kPa and 414 kPa respectively. A low pressure zone is created at immediate downstream of variable orifice. After that pressure recovery takes place. The size of low pressure zone increases with the increase in valve inlet pressure. This becomes clear from the stream function plots in Fig. 11. The plots clearly reveal the recirculation bubble and the associated downstream flow divergence in each case. Due to the increase in the size of the recirculation bubble with increase in the inlet pressure, the pressure recovery zone is pushed further right.

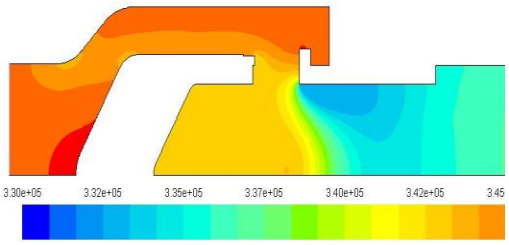

100% opening

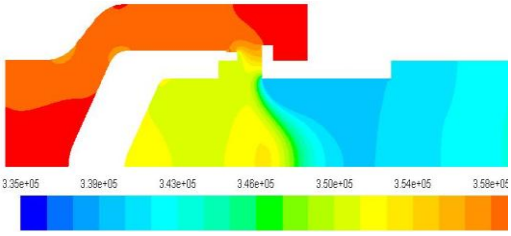

60% opening

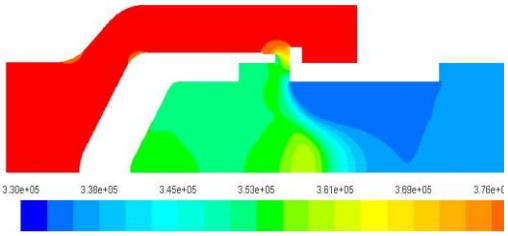

30% opening

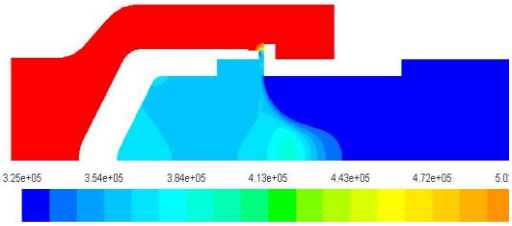

10%opening

Fig. 10. Pressure contour in Pascal in the main flow path of the valve.

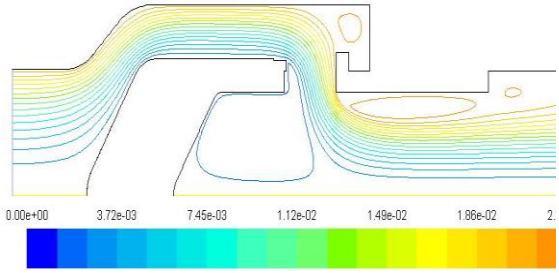

100% opening

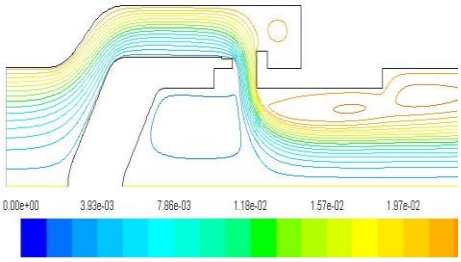

60% opening

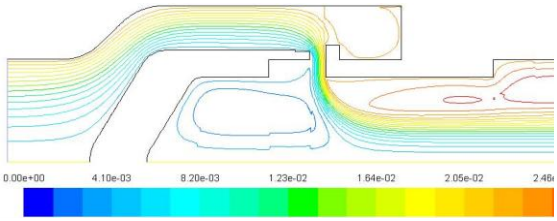

30% opening

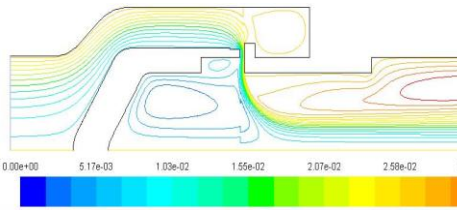

10% opening

Fig. 11. Contour of stream function (kg/s) inside the main valve.

Figs. 12 and 13 depict the variation of the Mach number and the velocity vector through the valve body and the initial part of the spool valve. The low values of these two variables in the valve body can be attributed to the higher mean radius of the valve body in comparison to the bore diameter of the spool valve. As expected these values also remain low in the regions of the three recirculation bubbles discussed above with reference to Fig. 11. Between the two recirculation bubbles inside the spool valve, the flow enters the spool valve almost in an inward radial manner. Consistent with the decrease in the flow area due to the decrease in the mean radius, both the Mach number and the velocity keep on increasing. These increases signifying flow acceleration continue even during the flow turning to almost axial direction. Near to the axis, the acceleration persists due to the small inward radial component. Away from the axis up to the bubble, the flow decelerates due its diverging nature owing to the small outward radial component. The location of the peak velocity region away from the axis can be attributed to the sharper turning of the flow and the corresponding acceleration prior to reaching this region. Because of the complex flow structure inside the valve discussed above, CFD prediction of spool flow forces is more reliable.

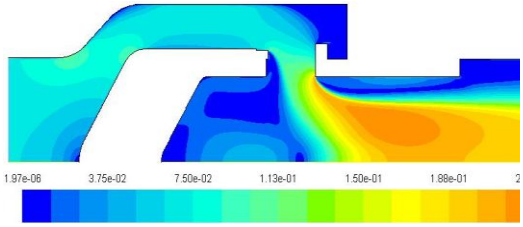

100% opening

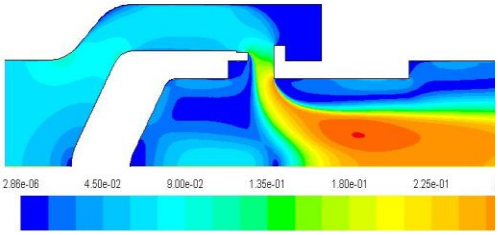

60% opening

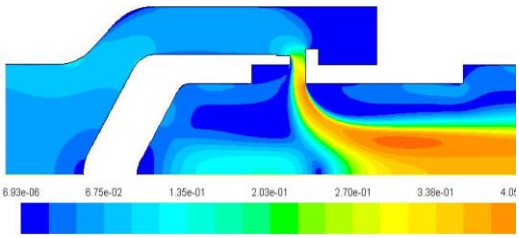

30% opening

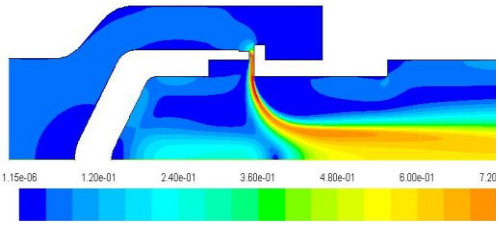

10% opening

Fig. 12. Contour of Mach number inside the main valve.

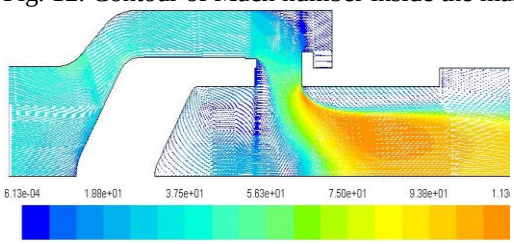

100% opening

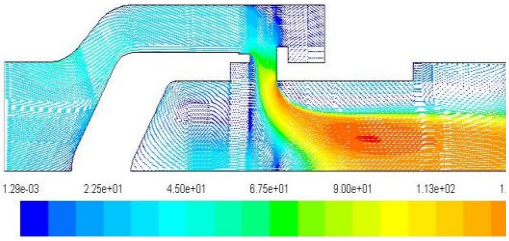

60% opening

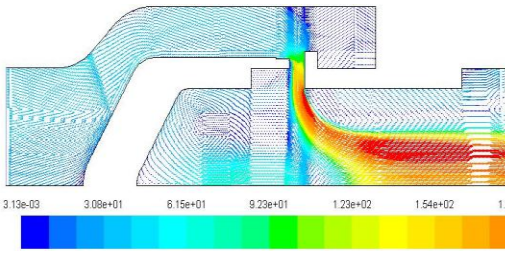

30% opening

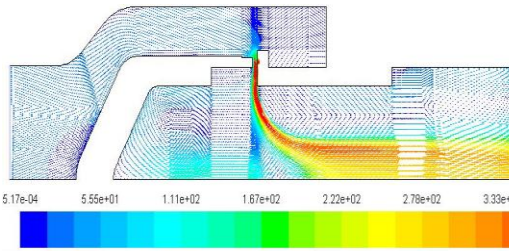

10% opening

Fig. 13. Velocity vector (m/s) inside the main valve.

V. CONCLUSION

Control circuit pressure characteristic has been calculated both analytically and by CFD method by solving compressible, turbulent flow through pressure regulated valve. In CFD analysis a special UDF has been developed to couple with ANSYS FLEUNT primarily to modify structured mesh of the flow domain dynamically with change in valve inlet pressure. CFD results has predicted better characteristic. Also, the simulation provides valuable insight into the control circuit behaviour, which is crucial for designers. Attempt to simulate using fully three-dimensional geometry is underway.

ACKNOWLEDGEMENT

We are thankful to Dr. Amitava Dasgupta for providing valuable advice on the functional aspect of the valve. Access to the high performance computing facility of CSIR-CMERI is gratefully acknowledged.

REFERENCES

[1]. Z. Leutwyler and C. Dalton. A computational study of torque and force due to compressible flow on a butterfly valve disk in mid-stroke position. J Fluid engineering, 128:1074-84, 2006.

[2]. R. Amirante, G. Del Vescove and A. Lippolis. Flow forces analysis of open center hydraulic directional control valve sliding spool. Energy Conversion and Management, 47:114-31, 2006.

[3]. R. Amirante, G. Del Vescove and A. Lippolis. Evaluation of the flow forces on an open centre directional control valve by means of a computational fluid dynamic analysis. Energy Conversion and Management, 47:1748-60, 2006.

[4]. R. Amirante, P.G. Moscatelli and L.A. Catalano. Evaluation of the flow forces on a direct (single stage) proportional valve by means of a computational fluid dynamic analysis. Energy Conversion and Management, 48:942-53, 2007.

[5]. M.J. Chern, C.C. Wang and C.H. Ma. Performance test and flow visualization of a ball valve. Experimental thermal and fluid sciences, 31:505-12, 2007.

[6]. H. Chattopadhyay, A. Kundu, B.K. Saha and T. Gangopadhyay. Analysis of Flow Structure inside a Spool Type Pressure Regulating Valve. Energy Conversion and Management, 53:196-204, 2012.

[7]. X.G. Song, J.H. Jung, H.S. Lee, D.K. Kim and Y.C. Park. 2-D dynamic simulation of a pressure relief valve by CFD. Proc. 9th WSEAS Int. Conf. on Applied Computer and Applied Computational Science, Hangzhou, China. April 11-13, 2010.

[8]. M. Borghi, M. Milani and R. Paoluzzi. Stationary axial flow force analysis on compensated spool valve. Int J fluid power, 1:17-25, 2000.

[9]. J. Deng, X.M. Shao, X. Fu and Y. Zheng. Evaluation of the viscous heating induced jam fault of valve spool by fluid-structure coupled simulations. Energy Conversion and Management, 50:947-54, 2009.

[10]. www.ansys.com

[11]. P.L. Skousen. Valve Handbook. New York: McGraw-Hill, 2004.

[12]. ASM International. ASM Handbook, Volume 18. Friction, Lubrication and Wear Technology, 1992.

[13]. T.H. Shih, W.W. Liou, A. Shabbir, Z. Yang and J. Zhu. A new k- ε eddy-viscosity model for high Reynolds number turbulent flows–model development and validation. *Computers Fluids*, 24:227-38, 1995.